GEOLOGICAL AND ENVIRONMENTAL REMOTE SENSING LABORATORY

Department of Geology
University of Puerto Rico at Mayaguez

Undergraduate Research Project:

Dynamics of river plumes as detected with AVIRIS

Eidalia González Tosado
802-01-2849
Advisor: Prof.Fernando Gilbes
December 2, 2005

Abstract:

The main purpose of this study was to evaluate the dynamics of three river plumes in Mayaguez bay and determine the distinct characteristics between them using AVIRIS (Airborne Visible/Infrared imagine Spectrometer) sensor. AVIRIS is a hyper spectral sensor with 224 spectral bands, a range from 400 to 2500 nm, strip lines of 11 km wide and spatial resolution of 18m. The wide range of bands can provide improved capabilities for remote sensing of the more complex and turbid waters. The suspended sediments concentrations were obtained by water samples collected at 10 stations along the Mayaguez bay area. These samples were compared with reflectance values from the AVIRIS image. This data was used to obtain an empirical algorithm that uses this wide spectral range to identify areas with suspended sediment in the Mayaguez Bay area. The suspended sediment concentration image showed higher amount of sediments in the Añasco and Guanajibo plumes and smaller amounts in the Yaguez. The Añasco plume spread out farthest into the bay with a high suspended sediment concentration of 15.52 mg/l near the shore and 1.40mg/l farther out into the bay area. The Guanajibo plume had a unique shape because of wave movement that transports the sediments southward along the coast with a concentration of 5.46 mg/l. The Yaguez plume did not spread out far into the bay but remained close to the shore with a concentration of 5mg/l.

Keywords: Mayaguez Bay, AVIRIS, suspended sediment, sediment dynamics, rivers

Introduction and Statement:

Remote sensing has been a useful tool for detecting differences in ocean color produced by changes in suspended sediment concentrations due to rivers discharge. Changes in topography, weather, and human activities affect the behavior of sediment dynamics in coastal areas, like the Mayaguez bay.

The main rivers in Mayaguez Bay are the Añasco, Yagüez and Güanajibo (Morelock et al., 1993). The sediments from the rivers are deposited on the shore or remain suspended all throughout the bay producing changes in ocean color. The study area reflects spatial variations in suspended sediments because of the seasonal changes in river discharge. The Mayaguez area has an annual precipitation range of 200-250cm. From September through November there is more precipitation resulting with the maximum river discharge (Rodríguez, 2005). Agriculture and urbanization have increased these variations and are in part responsible for large changes in ocean color. In the early 70's more than 97% of the land area was used for agriculture that included coffee and sugarcane crops. Nowadays this agriculture area is being substituted with urban development increasing the population from 50,000 in 1973 to 150,000 in 1998 (Sotomayor et al., 2004 unpublished information).

The main purpose of this research project was to evaluate the dynamics of the three river plumes and determine the distinct characteristics between them using the AVIRIS (Airborne Visible/Infrared imagine Spectrometer) sensor.

On August 19, 2004 on board aircraft 909 the sensor AVIRIS and Cirrus Digital Camera System (DCS) flew over Puerto Rico obtaining hyperspectral images of most of the coastline. AVIRIS (Airborne Visible/Infrared imagine Spectrometer) is a

hyperspectral sensor with 224 spectral bands, a range from 400 to 2500 nm, strip lines of 11 km wide and spatial resolution of 4m or 20m.

Figure 1. Map of Puerto Rico with the areas covered by AVIRIS in August 19, 2004 (Flight Summary Report Guild, NASA Ames Research Center, 2003).

This research project used the valuable information obtained by AVIRIS on this rainy day to detect differences in the three main river plumes (Río Añasco, Río Guanajibo, and Río Yaguez) by comparing discharge, and sediment dynamics. A reliable method that included the proper combination of bands to better understand the sediment dynamics in the Mayaguez bay was developed.

Literature Review:

Several research projects have been conducted in Mayaguez Bay using remote sensing. They have evaluated water quality, salinity, turbidity, phytoplankton, and river discharge. For example, several years ago a joint project with researchers from NASA-Stennis Space Center and the University of Puerto Rico at Mayagüez intended to use remote sensing for a better understanding of the land-sea interface in the west coast of Puerto Rico but the lack of technology made it difficult (Miller et al., 1994). Other studies have followed like when Gilbes et al. (1996) studied how the variation in river discharge of the western Puerto Rico affects the dynamics of phytoplankton in coastal waters. The study included nine stations that were sampled at three inshore-offshore transect involving the mouths of the Guanajibo, Yagüez and Añasco rivers to oceanic waters.

From March 1990 to February 1991 samples were collected monthly to determine variations in Chlorophyll-*a (Chl-a)*, salinity and suspended particles in the Mayagüez Bay. The highest concentrations of Chl-a were in August, September and January. The inshore transects had the highest concentration of Chl-*a*. Furthermore, the Añasco and Yagüez rivers had higher concentrations of Chl-*a* than the Guanajibo. Maximum concentrations for the Añasco and Yagüez transects were detected in August and for Guanajibo in October and November. Low salinity in the bay area is caused by high amount of fresh water in the wet season (September-November). During this period there is also an increase in the rivers discharge. The differences in Chl-*a* concentration imply

differences in nutrients, suspended sediments and freshwater run-off affecting coastal phytoplankton dynamics. High Chl-*a* was correlated with high-suspended particulate matter that is carried along with nutrients favorable for phytoplankton growth. Along with these results the light penetration was reduced and salinity concentrations were low (Rodríguez et al. 2005). The findings by Gilbes et al. (1996) demonstrate the important role of rivers discharge in the Mayaguez Bay. Therefore, it is important to study the dynamics of these river plumes and evaluate their unique sedimentary characteristics.

The spatial distribution of suspended sediments for Mayagüez Bay using traditional *in situ* measurements and remote sensed data was estimated by Miller et al. (1994). Otero et al. (1992) also used remote sensing to examine the effects of the Añasco, Yagüez and Guanajibo rivers on the phytoplankton production. They determined that *in situ* measurements of sea surface properties combined with airborne imagery were adequate to study the spatial and temporal dynamics of phytoplankton and suspended transport (Rodríguez et al. 2005).

Quiñones et al. 2005 indicated that the high concentration of suspended particles found in the Mayaguez Bay during the rainy season cause turbidities in the water that increase scattering and absorption, effectively attenuating light. During the wet season, the Añasco River shows high discharge and it is very important for phytoplankton due to the amount of nutrients that arrive to the coast (Quiñones et al. 2005). Morelock et al. (1983) indicate that the reefs in Mayaguez Bay are affected due to increasing sediment load from the rivers.

Since the late 1970's remote sensing studies of suspended sediments have been made knowing the fact that suspended sediments increase the radiance emergent from surface waters in the visible and near infrared region of the electromagnetic spectrum (Ritchie and Schiebe et al. 2000). Most researchers that had large ranges (i.e., 0-200+ mg/l) of suspended sediment concentrations have found a curvilinear relationship between suspended sediments and radiance or reflectance (Ritchie et al. 1976, 1990; Curran and Novo et al. 1988) because as suspended sediments increase the amounts of reflected radiance tend to saturate. The point of saturation depends on wavelength, with the shorter wavelength saturating at lower concentrations. Ritchie et al. (1976) using in situ studies concluded that wavelength between 700 and 800 nm were most useful for determining suspended sediments in surface waters. Many researchers have studied algorithms that separate sediment areas from shallow water areas using a combination of reflectance differences of the 0.55 μm, 0.66 μm, and 0.86 μm channels form MODIS data. This sensor has been highly used by researchers that study suspended sediment concentrations. MODIS is accepted among researchers because it is a multispectral sensor with 32 spectral bands that can be applied to a variety of remote sensing applications. This is why it is believed that AVIRIS a hyper spectral sensor with 224 spectral bands, a far more powerful sensor can also become an important tool for determining suspended sediments in surface waters in the Mayaguez Bay.

Methodology:

The plumes in Mayaguez bay were studied using AVIRIS (Airborne Visible/Infrared imagine Spectrometer) images collected during August 19, 2004. The images were used for developing a methodology to study the plumes of the Añasco, Guanajibo, and Yaguez rivers.

This study focused on the red and infrared bands to determine differences in ocean color produced by suspended sediments because this range of bands take advantage of the strong water absorption at wavelengths longer than 1000nm that don't allow illumination of sediments in the water or a shallow ocean floor (Li et. al. 2003). Changes in optical properties along the plumes were evaluated using the AVIRIS images. The image processing was performed using the software called ENVI (Environmental of Visualization Images) and ACORN (Atmospheric COrrection Now). It included atmospheric correction, specific algorithms testing for estimation of suspended sediments and creating a suspended sediment concentration image of Mayaguez bay.

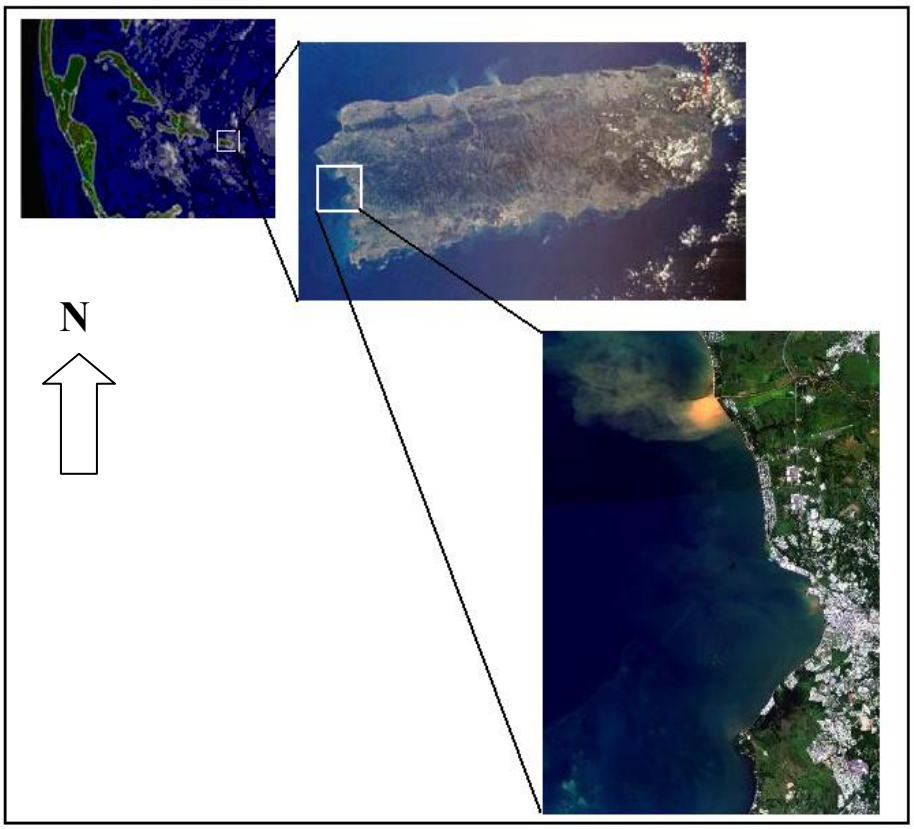

Figure 2. Study area: AVIRIS True color Image of the Mayaguez bay area (provided by Prof. Gilbes).

AVIRIS is a high-quality sensor for detecting changes in ocean color produced by suspended sediments because it is a hyperspectral sensor with high spatial resolution (17 meters). This hyper spectral sensor provides high dimensions of spectral patterns as well as high spectral resolution that make it possible to separate more classes (real differences in materials in subtle spectral shape differences). As shown in Figure 3 AVIRIS spectral

abilities are superior to those of Landsat Thematic Maper, which is a multispectral sensor with 7 spectral bands and a spatial resolution of 30 meters.

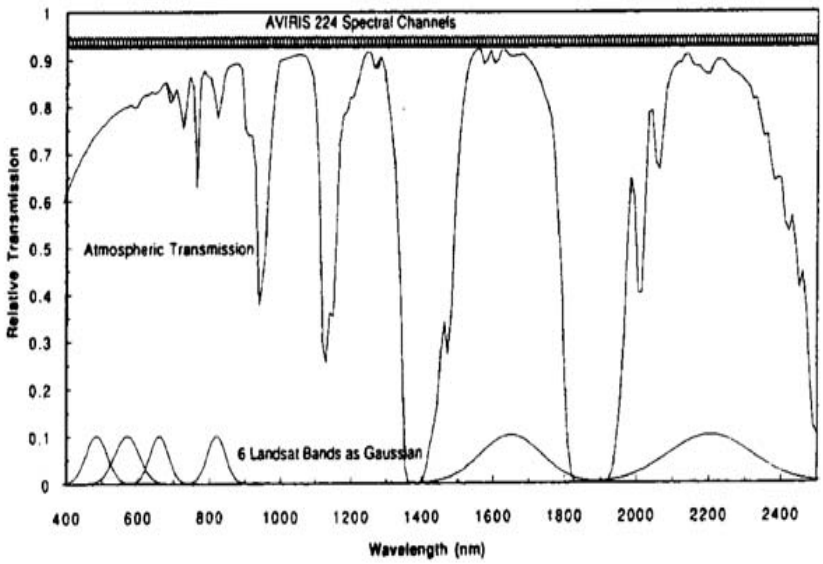

Figure 3. AVIRIS spectral channels compared to Landsat Thematic Maper spectral channels. The 220 narrow bands at the top represent AVIRIS spectral channels. For comparison, Landsat TM channels are shown at the bottom (Green and Simmons et al. 1993.

Field Work:

Field data was obtained during a cruise trip in Mayaguez Bay on August 19, of 2004 while the AVIRIS sensor was passing over the region. The sampling was done during the wet season from inshore to offshore waters, covering the Añasco, Yaguez, and Guanajibo rivers, and the regions affected by the dumping of the sewage pipe (Figure 4). Along with the sample collection, latitude and longitude of the samples were determined (using a GPS set) (Quiñones et al. 2005).

Station	Latitude	Longitude
S01	18° 16.00'	67° 12.00'
S02	18° 16.00'	67° 13.10'
S04	18° 16.00'	67° 15.20'
S05	18° 14.40'	67° 11.40'
S07	18° 14.40'	67° 13.50'
S13	18° 12.20'	67° 09.78'
S15	18° 12.20'	67° 11.95'
S21	18° 10.25'	67° 11.10'
S23	18° 10.25'	67° 13.15'
S24	18° 10.25'	67° 14.80'

Table 1. Latitude and Longitude of Sampled Stations.

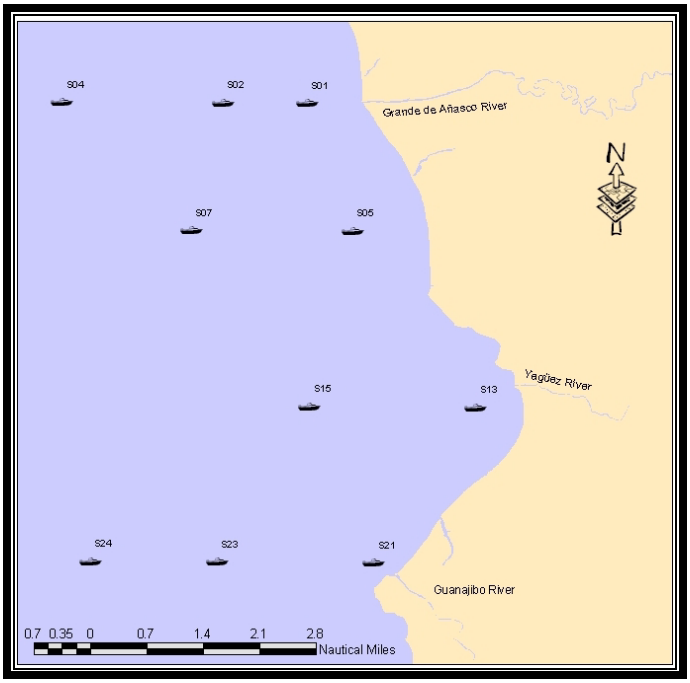

Figure 4. Study area with 10 sampled areas (Quiñones, 2005).

Also the ten stations were sampled with the bio-optical rosette. This rosette is made up of several instruments that measure the different bio-optical properties of the water column. Coastal areas have large spatial variability of bio-optical properties; that is why this methodology allows measuring this variability more efficient and accurate because all the instruments are collecting profiles of data at the same time and from the same water parcel (Quiñones, 2005).

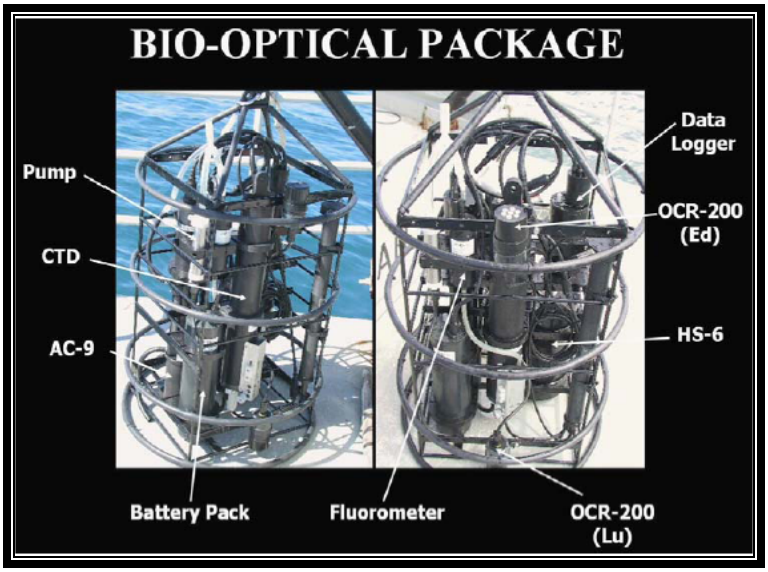

Figure 5. Customized rosette with different bio-optical instruments.

A CTD (Seabird SBE-19 with pump) measured salinity and temperature. The spectral transmittance, c (λ), and spectral adsorption, a (λ), was measured over nine wavelengths with the AC-9 meter (from Wet Labs). The backscattering coefficient, Bb (λ), at six wavelengths was measured with the HydroScat-6 (from Hobi Labs). Upwelling radiance, L_u (0-, λ), and downwelling irradiance, E_d (0-, λ), was obtained using a submersible radiometer (Model OCR-200 from Satlantic).

Water samples were obtained from the 10 stations at two depths. Then the collected samples were taken to the laboratory to obtain suspended sediment concentration. This was determined using the standard weight difference method. This data was used for quality assessment of the image.

Lab Work:

Image processing:

- The AVIRIS images from transects A-B and C-D along the Mayaguez bay were selected for the study (Figure 1).
- Using ACORN (Atmospheric COrrection Now) a simple atmospheric correction was produced for the two images. An ACORN User's guide was developed for future use of the program with AVIRIS images (Appendix B).
- Using ENVI (Environmental of Visualization Images) regions of interest were developed in a 5x5 pixel range for each of the 10 stations using the latitude and longitude data.
- Spectral data (reflectance vs. wavelength) was obtained from each region of interest as well as three individual points for the Añasco, Guanajibo and Yaguez river plumes to create a Reflectance vs. Wavelength graph and look for relationships between the bands and suspended sediment concentrations. (Figure 6).
- The spectral data (reflectance vs. wavelength) for each station was organized with Microsoft Excel software.
- Based on previous works a group of 20 bands from the red and infrared spectrum (500-787nm) were selected to compare reflectance values with suspended sediment concentration from the water samples collected.
- Graphs of Suspended Sediment Concentration vs. Reflectance were developed to acquire an algorithm with a good correlation value (R^2). The best algorithm was obtained from band 46 (777nm).
- This algorithm was entered into ENVI (Environmental of Visualization Images) to create a suspended sediment concentration images.
- A mask for the obtained suspended sediment concentration image was created to distinguish between turbid sediment waters and clear waters.

- Both images from transects A-B and C-D along the Mayaguez bay were selected to create a mosaic with both images. Then the algorithm and mask were applied to create the final image.

Results:

The red and infrared bands were used to determine differences in ocean color produced by suspended sediments. Using three reflectance values for each River plume a graph was developed to observe the behavior of the curves.

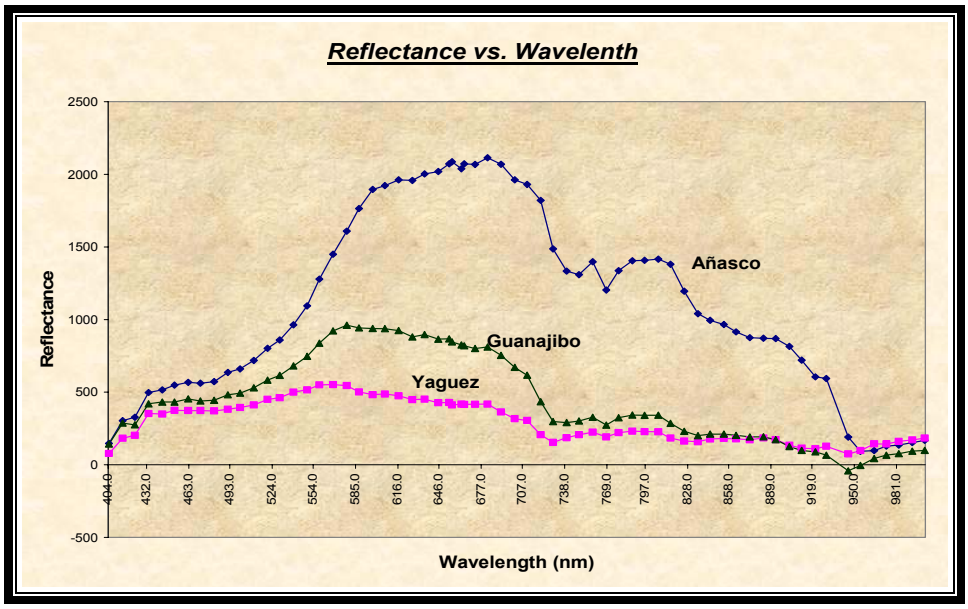

Figure 6. Reflectance vs. Wavelength for the Añasco, Yaguez and Guanajibo.

The 20 bands located in the red to infrared (500-787) spectrum were used to obtain good correlation values with suspended sediment concentrations obtained from the water samples (Appendix A). The density of the collected samples was as low as 1.13 and as high as 16.72 mg/l. The water samples from station 5 (16.72 mg/l) was not used because it is located far from the coast where there is low suspended sediment concentration.

The results shown in Table 2 indicate the number of bands, the algorithm coefficients, and value of correlation (R^2) used to obtain the final suspended sediments concentration algorithm.

Band	**Wavelength(nm)**	**a**	**b**	**Value of Correlation (R^2)**
15	500.8	0.04	-9.77	0.58
16	510.5	0.03	-6.65	057
17	520.2	0.03	-6.27	0.75
18	529.8	0.02	-5.00	0.74
19	539.5	0.02	-4.21	0.74
20	549.0	0.02	-3.02	0.76
21	558.7	0.01	-1.89	0.73
22	568.3	0.01	-1.39	0.76
23	578.0	0.01	-0.62	0.74
24	587.6	0.01	0.42	0.77
38	701.2	0.02	1.96	0.74
39	710.6	0.03	1.80	0.75
40	720.2	0.04	2.43	0.75
41	729.8	0.07	2.24	0.80
42	739.3	0.08	0.99	0.81
43	748.9	0.08	0.51	0.80
44	758.5	0.07	0.40	0.80
45	768.0	0.10	0.85	0.89
46	777.6	0.08	0.03	0.82
47	787.2	0.08	-0.14	0.82

*suspended sediment concentration (mg/l) = **a** (x) + **b**.

Table 2. Bands, algorithm coefficients and values of correlation.

Graphs were developed between suspended sediment concentrations from the water samples and reflectance from each of the 20 bands. Nonetheless, only the bands with high values of correlation were used to develop the algorithm.

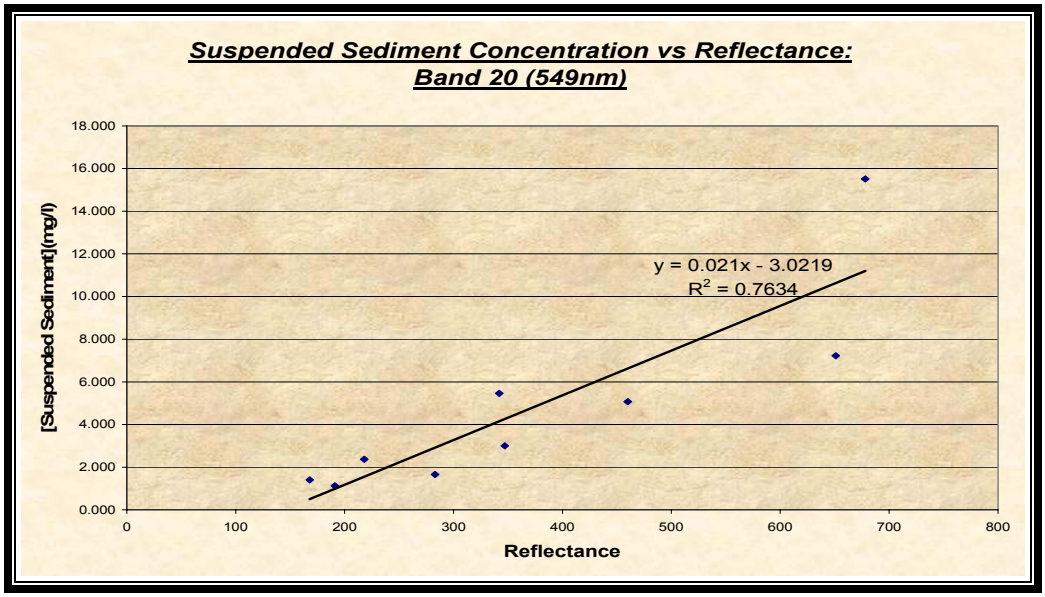

Figure 7. Suspended Sediment Concentration versus Reflectance in the 549.1nm band 20.

A linear fit was run with the visible spectrum data in 549nm with a value of correlation (R^2) of 0.764 (Figure 9). The fitted line has the equation of:

Suspended Sediment Concentration (mg/l) = a (x) + b; where **a** equals 0.021, **b** is –3.0219 and **x** is the reflectance of band 20 (549nm).

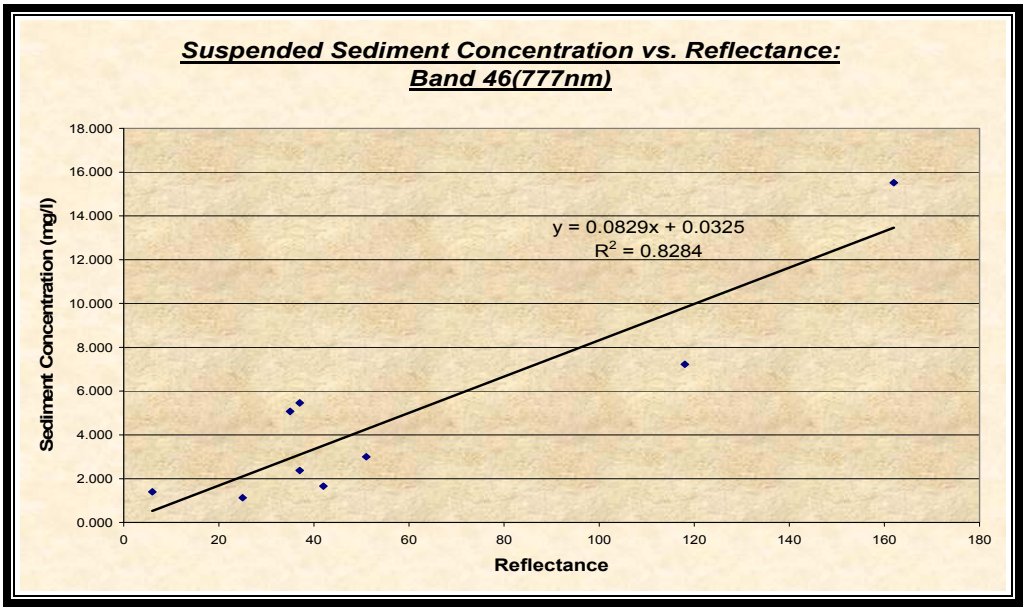

Figure 8. Suspended Sediment Concentration versus Reflectance in Band 46 (777nm).

A linear fit was run with the visible spectrum data in 777nm with a value of correlation (R^2) of 0.82 (Figure 10). The fitted line has the equation of: Suspended Sediment Concentration (mg/l) = a (x) + b; where **a** equals 0.0829**, b** is 0.0325 and **x** is the reflectance of band 46 (777nm).

A suspended sediment concentration image was developed using the algorithm obtained from band 46 (777nm).

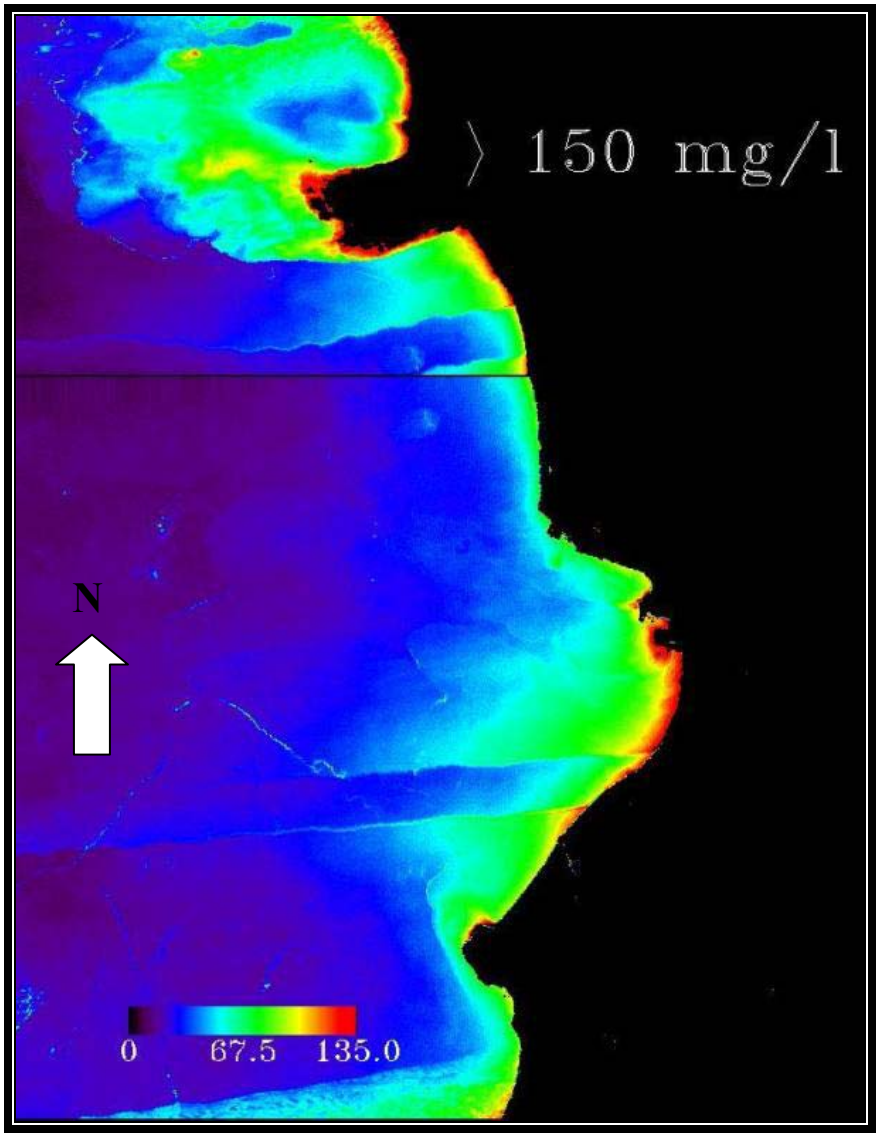

Figure 9. Suspended Sediment Concentration Image of the Mayaguez Bay area.

Using the Image data suspended sediment concentrations were compared between the water samples and selected bands.

Station	[SS] Field Data	[SS] Band 20(549nm)	[SS] Band 46(777nm)
S01	15.52	12.90	14.54
S02	7.22	8.44	6.75
S04	1.40	0.59	1.02
S05	16.72	3.95	3.18
S07	2.37	1.19	2.18
S13	5.07	7.14	4.59
S15	3.00	4.18	2.85
S21	5.46	6.15	3.26
S23	1.66	2.15	2.10
S24	1.13	0.98	1.44

Table 3. Suspended Sediment Concentrations (mg/l) for each station.

Discussion and Interpretation:

Mayaguez Bay is a dynamic environment that involves the continuous deposition of sediments from the three main river; Añasco, Yaguez and Guanajibo. However, the Añasco River is the main supplier of sediments into the bay because it has a larger basin than the Yaguez and Guanajibo Rivers. The River plumes are formed when the amount of sediments transported into the ocean becomes larger than ocean erosion can carry away. Especially in periods of heavy rain fall (August to November).

The image taken on August 19, 2004 shows changes in ocean color especially near the Añasco river mouth; indicating large amounts of discharge. Daily discharge data was obtained for the Añasco River to compare with suspended sediment concentrations in the study area. The USGS daily discharge graph shows a peak between August 17 and August 19 indicating high discharge when compared with the median daily stream flow based on 40 years of record.

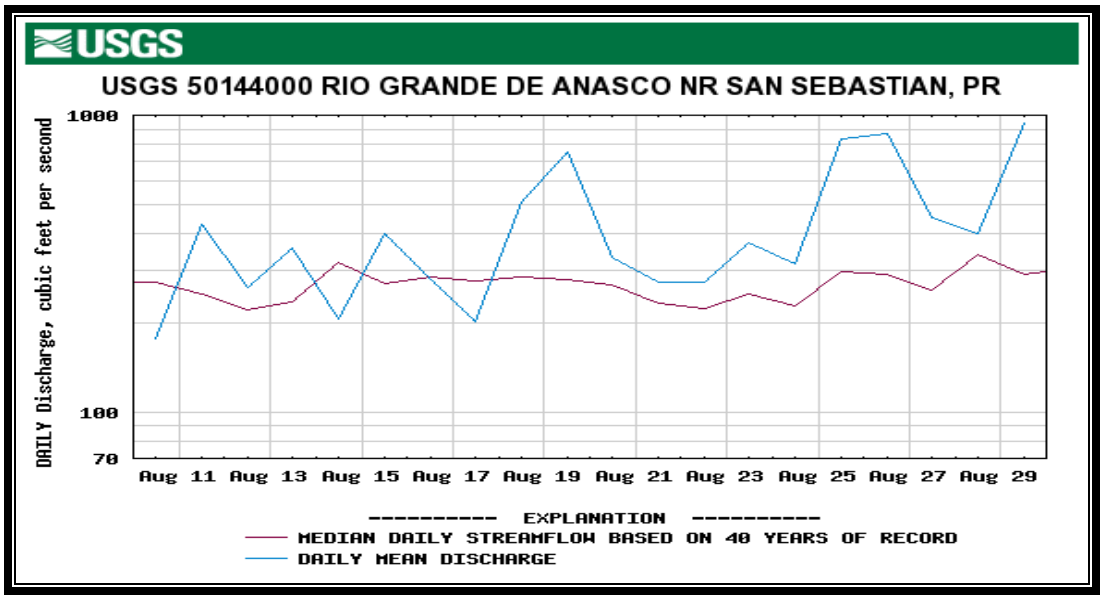

Figure 10. Daily Discharge vs. August of the Rio Grande de Añasco from the USGS Real-Time Water data (http://waterdata.usgs.gov/pr).

The sediments that are found at the mouth of the Añasco River watershed are mostly pebbles to silt that indicate the sediments traveled a long distance. The sediments found at the beach tend to be finer sediments because they are constantly being reworked by the waves not letting the sediments settle at the bottom of the channel and leaving them in suspension (Rodriguez et al. 2005).

The selected band was 46 (777nm) because of its high correlation value even though it did not have the highest R^2 of all the 20 bands. The highest value of correlation was found on band 45 (768nm) which was 0.89 but this was obtained using only 9 stations and 9 reflectance values. Band 46 used 9 stations and 10 reflectance values. The minimum suspended sediment concentration that could be detected was from 0 mg/l to 25 mg/l. This makes the algorithm suitable for detecting coastal turbid waters, while using relatively low spatial resolution sensors such as AVIRIS.

When the water samples and the final suspended sediment concentration image were compared a good correlation was obtained. The suspended sediment concentration image showed higher amount of sediments in the Añasco and Guanajibo plumes and smaller amounts in the Yaguez. The Añasco plume spread out farthest into the bay with a high suspended sediment concentration of 15.52 mg/l near the shore and 1.40mg/l farther out into the bay area. The Guanajibo plume had a unique shape because of wave movement that transports the sediments southward along the coast with a concentration of 5.46 mg/l. The Yaguez plume did not spread out far into the bay but remained close to the shore with a concentration of 5mg/l.

Since the Añasco River is the principal sediment supplier into the ocean there is a unique hydrodynamic interaction between the river's fresh water and seawater as well as differences in density produced by sediment load, and wave and current action in the ocean. A sharp contrast between water densities exist where less dense fresh water enters the denser saline seawater. The river plumes look like a plane jet that spreads out and forms a layer over the seawater. However, if the stream water has high suspended load, it

may be denser than the water it is flowing into, and it will quickly sink to the bottom, leaving only a small sediment plume visible on top (Prothero,1996). The spreading distance of the plume depends on the frictional inertia between the freshwater and seawater. Because there is limited mixing in the boundaries of the jet, there is relatively little frictional inertia. That is why the jet goes a long way seaward before freshwater breaks up and mixes with sea water. The sediments that were carried in the stream are deposited along the sides of the jet in sub aqueous levees where friction and mixing slow the flow down. The jet slows down farther offshore because of friction and spreading; depositing the sediments in mouth bars but the finest suspended matter is carried even farther creating changes in ocean color. The shape of the plume will depend on the rate of sediment influx relative to the wave and current energy of the sea (Easterbrook,1999). Most of the sediment influx into higher-energy coastlines is distributed laterally along the shoreline by wave action; like the Guanajibo plume.

The results from the image processing were compared with field data collected during the same day the image was collected. Including salinity, suspended sediments, chlorophyll-a, and optical properties (Quiñones et al. 2005). The salinity map showed lower values near the river mouths where fresh water reached the seawater. The salinity data was affected by the backscattering produced by suspended sediments in the water that indicate large amounts of suspended sediments in the Añasco and Guanajibo areas which correlates with the created image. Salinity and Temperature vary with depth. At deeper depth salinity is higher and temperature is lower. On the other hand at shallow depths salinity is less and temperature increases. Temperature influences the density of the fresh water introduced by the river affecting the distribution of the suspended sediments in the plume. If the fresh water is cold it will become denser and suspended particles will quickly sink to the bottom. Temperature maps showed a 1 degree differences between the Añasco plume and Yaguez and Guanajibo plumes. The temperature for the Añasco and Yaguez coasts were 28.8 ^{o}C and Guanajibo was 29.1^{o}C.

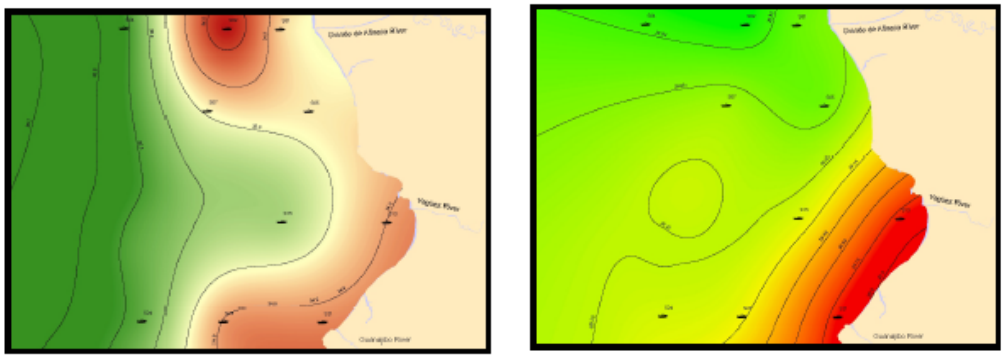

Figure 11. Left upper corner: Salinity (green color) was affected by the fresh water (red color) that comes from the rivers along the Mayagüez bay. Right upper corner: Shows that the higher temperature (dark color) comes from Yagüez and Güanajibo area than Añasco area although is approximately 1 grades of difference.

Do to high amounts of suspended sediments in the Añasco plume the phytoplankton population was high because of high concentrations of nutrients brought by the sediments; especially during the wet season.

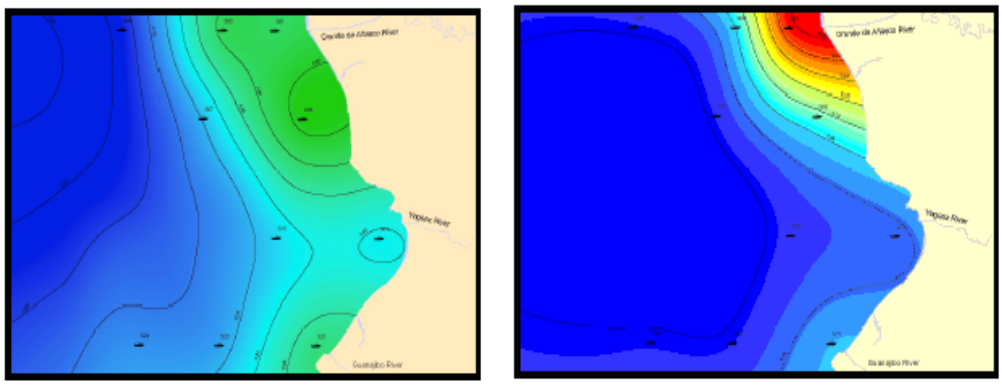

Figure 12. Left lower corner: Show a growth of phytoplankton population in Añasco and Güanajibo area in the rainy season, it observes the fluorescence (green color) product of chlorophyll-a. Right lower corner: Shows higher values of backscattering (wavelength 589) in the Añasco area by the high concentration of sediments that load the Añasco river in the rainy season (Quiñones et al. 2005).

Conclusions:

The principal factor for the diverse dynamics found on the Mayaguez bay is river discharge. River discharge from the three main rivers the Añasco, Yaguez and Guanajibo influence the dynamics and optical properties of the Bay. The Bay is influenced by the amount of deforestation and development that favor erosion and transference of soil particles into the river. These suspended sediments are transported into the bay causing turbidity in the water and differences in ocean color.

The suspended sediment concentration image shows various sediment dynamics present in the Mayaguez Bay area. The three main rivers showed distinct characteristics between them; discharge, spreading of the plume and suspended sediment concentrations. All these characteristics influence the dynamic of the sediments in each river plume. The suspended sediment concentration image showed higher amount of sediments in the Añasco and Guanajibo plumes and smaller amounts for the Yaguez. The Añasco plume spread out farthest into the bay with a high suspended sediment concentration of 15.52 mg/l near the shore and 1.40mg/l farther out into the bay area. The Guanajibo plume had a unique shape because of wave movement that transports the sediments southward along the coast with a concentration of 5.46 mg/l. The Yaguez plume did not spread out far into the bay but remained close to the shore with a concentration of 5mg/l.

The use of Remote Sensing helped develop a reliable algorithm demonstrating that remote sensing is a useful tool for detecting changes in ocean color produced by suspended sediments. The combination of bands did not entirely depend on the value of correlation as it was first expected but actually depended on the amount of field data available. For example, station 05 in band 45 (768nm) had the highest correlation value (R^2) but only used 9 of the 10 stations and 9 of the 10 reflectance values.

Further studies should be conducted using other sensors like MODIS because it was proven that the number of bands is not the most important aspect for suspended sediment detection. The most important factor would be the amount of field data used to

compare with reflectance values in the red and infrared range of the spectrum. As well as create an image of suspended sediment concentration for the whole island of Puerto Rico.

Summary:

An image was created from AVIRIS of Suspended Sediment Concentrations in the Mayaguez Bay area. Low concentrations of Suspended Sediments were related with areas of low discharge and were represented with minimum spreading of the river plume. High concentrations of Suspended Sediments were related to areas of high discharge and large distances of spreading throughout the bay area. The image was taken during a rainy day were discharge was at its highest and the rivers were covered with suspended sediments.

Several samples that were collected during this day were used to create the Suspended Sediment Concentration image. The samples of suspended sediments were obtained from 10 stations located in the Mayaguez Bay. Only 9 were used to compare with spectral reflectance data in the 20 bands used. The 20 bands ranged from 500nm to 800nm; which include the red and infrared bands. An algorithm was obtained from these comparisons to create a method for transforming the reflectance image into an image of Suspended Sediment Concentration. The algorithm obtained from band 46 (777nm) was used to create the image.

The Suspended Sediment Concentration image shows diverse sediment dynamics present in the Mayaguez Bay area. The three main rivers showed distinct characteristics between them due to discharge, spreading of the plume and suspended sediment concentrations. All these characteristics influence the dynamic of the sediments in each river plume. Using Remote Sensing helped develop a reliable method that included the proper combination of bands demonstrating that remote sensing is a useful tool for detecting changes in ocean color produced by suspended sediments.

References:

Curran, P.J. and Novo, E.M.M., 1988, The Relationship between Suspended Sediment Concentration and Remotely Sensed Spectral radiance: A Review.J. Coastal Res., 4(3), pp. 351-368.

Easterbrook, D.J., 1999, Surface Processes and Landforms 2nd edition, p.165-166.

Gilbes, F, López, J.M. and Yoshioka, P.M., 1996, Spatial and temporal variations of phytoplankton chlorophyll *a* and suspended particulate matter in Mayagüez Bay, Puerto Rico:Journal of Plankton Research, v. 18, p. 29-43.

Li, R.R., Y. J. Kaufman, B.-C. Gao, and C. O. Davis (2003). Remote sensing of suspended sediments and shallow coastal waters. *IEEE Trans. Geosci. Remote Sensing*, 41(3), 559-566.

Miller, R.L., Cruise, J.F., Otero, E. and López, J.M., 1994, Monitoring suspended particulate matter in Puerto Rico: Field measurements and remote sensing: Water Resources Bulletin, v.30, p. 271-282.

Morelock, J., Grove, K. and Hernández, M.L., 1993, Oceanography and patterns of shelf sediments Mayagüez, Puerto Rico: Journal of Sedimentary Petrology, v. 53, p. 371-381.

Otero, E., Miller, R.L. and López, J.M., 1992, Remote sensing of chlorophyll and sediments in coastal waters of Puerto Rico: Presented at the First Thematic Conferences on Remote Sensing for Marine and Coastal Environments, New Orleans, Louisiana, USA.

Prothero, D.R., and Schwab, F., 1996, Sedimentary Geology, p.169-180.

Quiñones, J.A., 2005, Bio-optical Variability in Mayaguez Bay during the Rainy Season: Undergraduate Research, University of Puerto Rico at Mayaguez, Geology Department.

Ritchie, J.C. and F.R. Schiebe 2000, Remote Sensing in Hydrology and Water Management, *Water Quality*, In: G.A. Schultz and E.T. Engman (eds.) Springer-Verlag, Berlin, Germany, pp. 287-303,305-353.

Ritchie J.C. and Cooper, C.M.., 1988, Comparison of Measured Suspended Sediment Concentration with Suspended Sediment Concentrations Estimated from Landsat MSS data. International Journal of Remote Sensing. Vol.9 No. 3, pg. 379-387.

Ritchie, J.C., Schiebe, F.R., and McHenry, J.R.; 1976, Remote Sensing of Suspended Sediments in Surface Water, Photogrammetric Engineering and Remote Sensing, Vol. 42, No.2 pp. 1539-1545.

Rodríguez, K., 2005, Determination of the Origin of the Sediments Discharge by the Río Grande de Añasco: Undergraduate Research, University of Puerto Rico at Mayaguez, Geology Department.

Acknowledgments:

I would like to thank Dr. James Goodman from the CID of the University of Puerto Rico at Mayaguez for giving me the AVIRIS images of the Mayaguez Bay area and for helping me understand ACORN better. I have to thank Wilfredo Alequín for setting up the GERS lab for me. Thanks to my advisor, Dr. Fernando Gilbes for answering all my questions.

Appendix:

Appendix A:

				1	2	3	4	5	6	7	8	9	10
Stations	Sediment Concentrations (mg/l)		Wavelength	701.0701	710.639	720.2094	729.7812	739.3546	748.9296	758.506	768.0839	777.6635	787.2444
S01	15.520		Reflectance	356	332	218	147	154	159	165	130	162	169
S02	7.220			308	281	172	105	109	112	120	91	118	125
S04	1.400			0	4	-21	-22	4	6	8	-6	6	11
S05	16.720			32	32	3	0	25	29	31	16	37	40
S07	2.370			6	10	-15	-13	14	21	24	16	35	38
S13	5.070			69	64	22	12	40	51	53	31	51	55
S15	3.000			45	48	7	-1	27	32	35	19	37	39
S21	5.460			32	31	4	-3	28	35	40	25	42	43
S23	1.660			22	28	0	-9	17	24	24	10	25	29
S24	1.130			10	19	-12	-12	9	15	14	0	17	17
			Wavelength	500.895	510.5325	520.1711	529.8109	539.4518	549.094	558.7373	568.3818	578.0275	587.6743
S01	15.520		Reflectance	511	523	573	585	630	678	730	766	742	691
S02	7.220			500	508	549	567	617	651	717	732	734	666
S04	1.400			274	219	223	205	203	168	166	145	113	71
S05	16.720			334	315	340	323	328	318	322	291	261	195
S07	2.370			274	248	251	236	240	218	204	190	147	108
S13	5.070			401	399	433	428	450	460	498	492	427	337
S15	3.000			350	333	345	338	353	347	350	333	300	217
S21	5.460			327	326	346	330	336	342	319	308	254	196
S23	1.660			328	296	316	300	305	283	273	255	208	142
S24	1.130			245	241	233	212	211	191	175	158	131	83

Table A. The Suspended Sediment Concentration for each of the ten stations and the two groups of wavelength with their respective reflectance values.

Appendix A: Acorn Users Guide

GEOLOGICAL AND ENVIRONMENTAL
REMOTE SENSING LABORATORY
Department of Geology
University of Puerto Rico at Mayaguez

Atmospheric Correction User's Guide: ACORN for AVIRIS

Student: Eidalia González Tosado
Email: eidalia_gonzalez@hotmail.com
Advisor: Dr. Fernando Gilbes
Email: gilbes@cacique.uprm.edu

ACORN:

1. Start ACORN.
2. Select Simple Atmospheric Correction for calibrated hyperspectral data (figure 1) and a Control File Editor window will appear (figure 2).

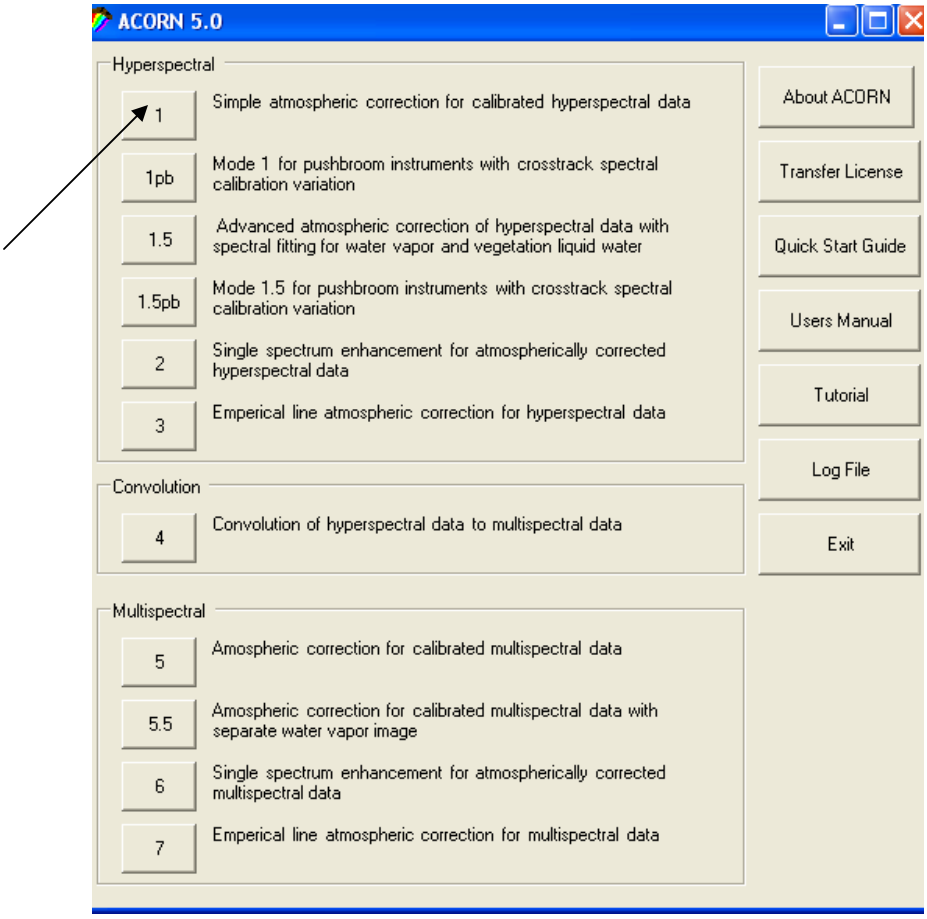

Figure 1. ACORN 5a Main Window

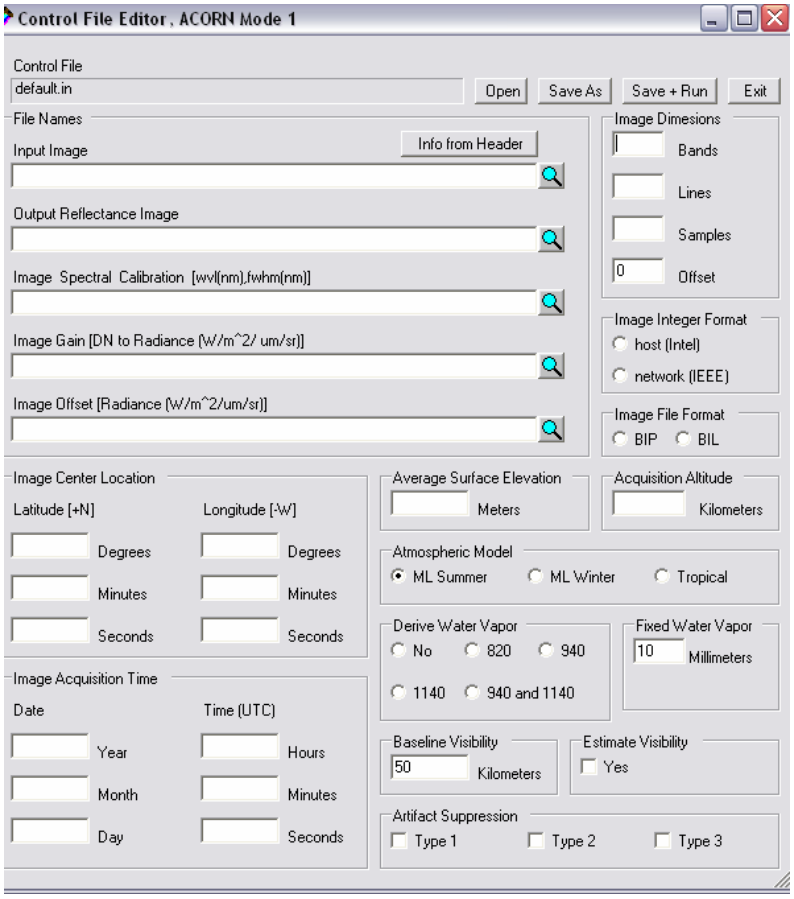

Figure 2. Control File Editor window

3. Select Input Image File Name (figure 3) which is the original geo referenced image file. For example: **C:\Documents and Settings\eidalia\My Documents\f040819t01p00r04c\f040819t01p00r04c_sc01_geo_img**

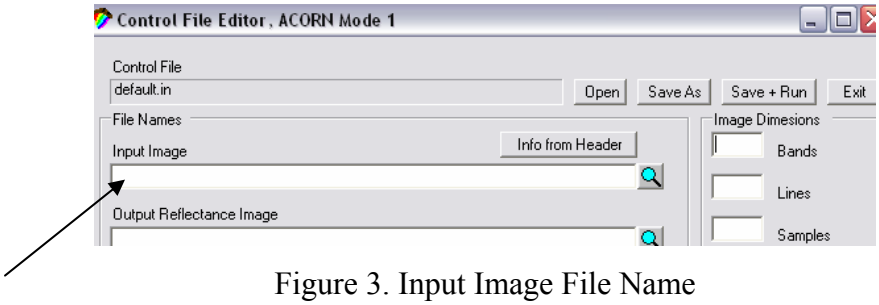

Figure 3. Input Image File Name

4. Select a name for the Output Reflectance Image file; this is basically the New Input Image File name (figure 4). For example: **C:\Documents and Settings\eidalia\MyDocuments\f040819t01p00r04c\f040819t01p00r04c_sc01_geo_img_acorn**

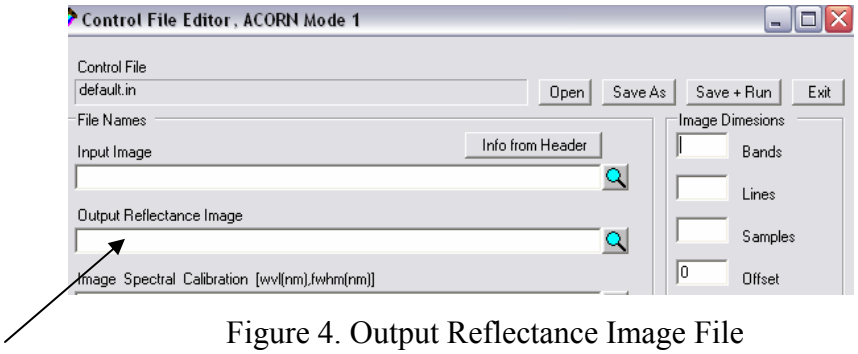

Figure 4. Output Reflectance Image File

5. Open the Image Spectral Calibration File (figure 5) will include wavelength and full weight half bands data from the original image this data will come in four columns but only the first two columns will be used. This file is found as a **.spc** file in each image files. For example: first column 366.09, second column 9.0852.

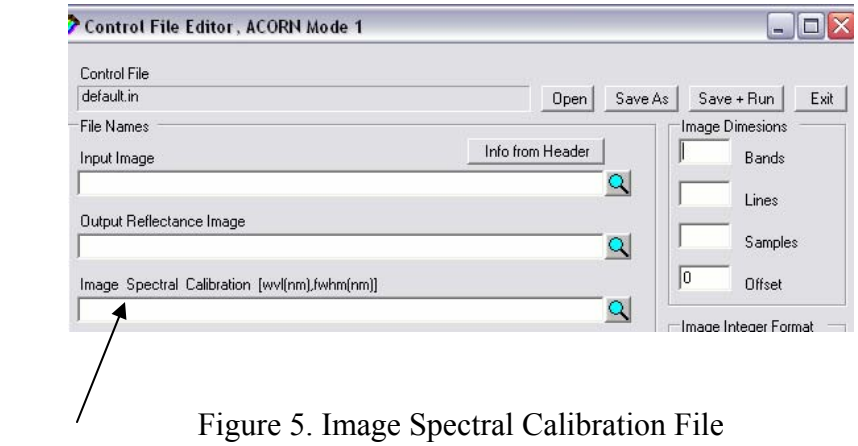

Figure 5. Image Spectral Calibration File

6. Open Image Gain File that will include radiance data (figure 6). The radiance data must be changed to an inverse form and converted to **µW/ cm^2 nm.sr** units. For example: **300 radiance → 1/300→0.00333 W/m^{2}µm·sr →0.00333 x 10 →0.0333 µW/ cm^2 nm.sr**

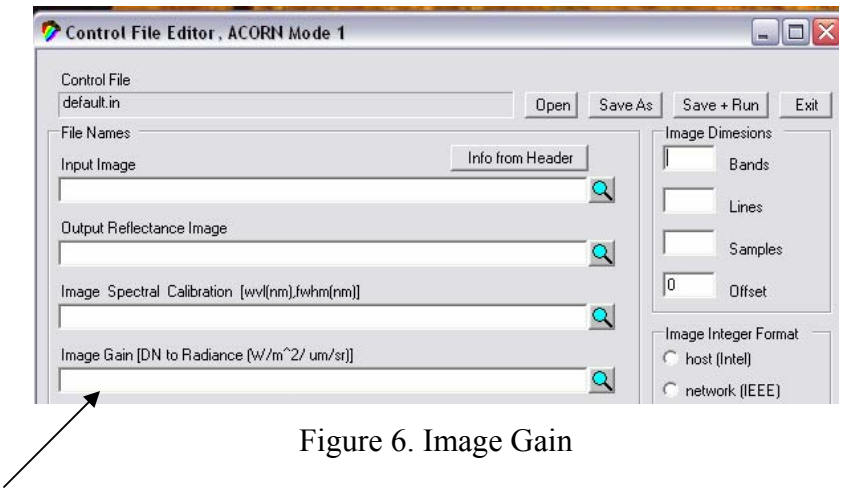

Figure 6. Image Gain

7. Open Image Offset File which includes a column of Zero's (figure 7). The Gain file is found in the Original image files.

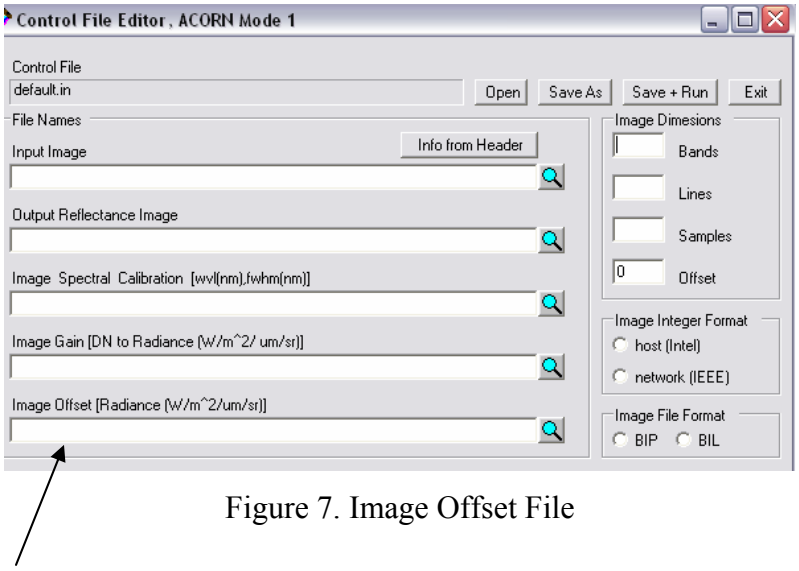

Figure 7. Image Offset File

8. Using the original Image Header fill in the Image Dimension window which includes number of bands, lines, samples, and offset (figure 8). For example: Bands 224, Lines 926. and Samples 2015.

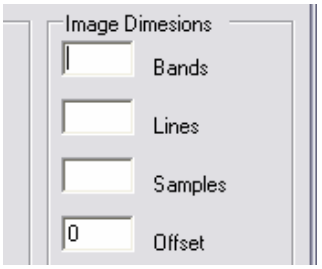

Figure 8. Image Dimension data

9. The Integer Format will depend on the image. Choose between host (Intel) and network (IEEE). Host (Intel) is selected when the computer used to process the image is part of a Host system. Network (IEEE) is used when the computer used to process the image is part of the network.

Figure 10. Integer Format

10. The Input File Format will depend in the image if it is bip or bil (figure 9) .This data is found in the Original Image Header.

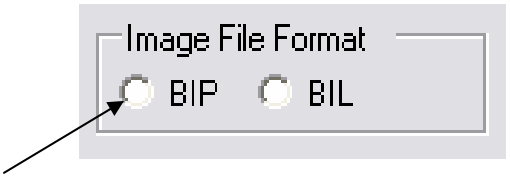

Figure 9. The Input File Format

11. The Image Center Location Data will include center latitude and longitude (figure 10). An Average of a center point in the image. If the direction of the Longitude is west it will be negative (Appendix A).

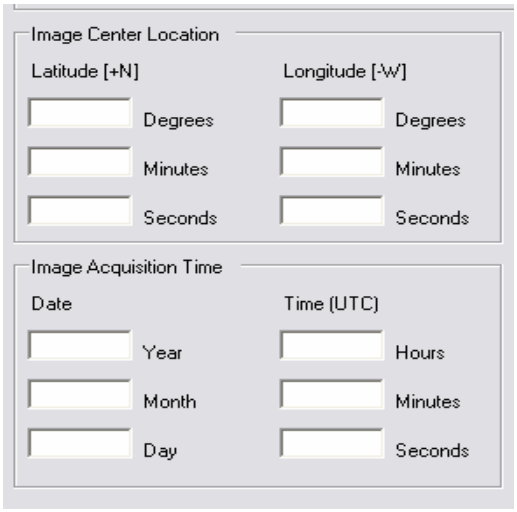

Figure10. Image Center Data

12. In the Image Acquisition section includes Date (figure 10) which includes day, month and year the image was taken (Appendix A). For example: August 19, 2004.
13. Time will be in UTC units which are the same as GMT units (Figure 10). It includes hours, minutes and seconds (Appendix A). For example: 13:36:45. The Average Surface Elevation will always be zero meters because it indicates mean sea level elevation (figure 10).

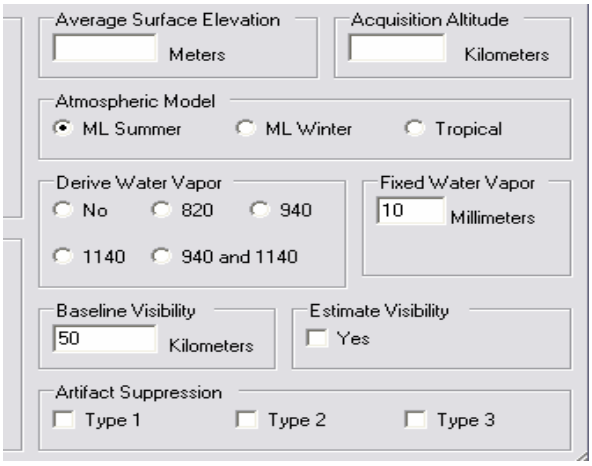

Figure 11. Image Mean Elevation, Image Acquisition Altitude, And Atmospheric Model, Derive Water Vapor, Fixed Water Vapor, Image Atmosphere Visibility and Artifact Suppression.

14. The Image Acquisition Altitude (figure 11) must be in kilometers (Appendix A).
15. The Atmospheric Model (Figure 11) will depend on the geographic location of the image. For Example: For images taken in Puerto Rico select Tropic.
16. The Derive Water Vapor (Figure 11) includes a series of wavelength that are derived on a pixel by pixel basis depending on the Image Sensor. For example: for AVIRIS select Both 940 and 1140. The Fixed Water Vapor will depend on the Image data. For example: 20 Millimeters.
17. Image Baseline Visibility (Figure 11) can be any number because ACORN estimates Visibility. Select **Yes** in the ACORN Estimated Visibility box. For example: 20 Kilometers.
18. In the Artifact Suppression box there are three types: Type 1, Type 2, and Type 3 (Figure 11).
    a. Type 1 Artifact suppression Type 1 attempts to assess and correct for any mismatch in the spectral calibration of the hyperspectral data set and the spectral radiative transfer calculations. This suppresses the artifacts (sharp spikes) near the strong atmospheric absorption features at 760,940, 1150, 2000 DID.
    b. In Type 2 there are often some other small artifacts across the spectral range due to errors in the absolute radiometric calibration and/or errors in the radiative transfer calculations. Artifact suppression type 2 attempts to suppress these.
    c. In Type 3 the portions of the spectrum across the 1400 and 1900 nm water vapor bands typically give very noisy reflectance results. These noisy values result from the low radiance values in these portions of the spectrum. ACORN artifact suppression type 3 assesses the signal levels of the calibrated radiance and suppresses the lowest signal portions where erroneous reflectance calculations may occur. The result is that low signal portions of the spectrum are set to zero on the reflectance output. Figure 3-3 d shows the result of ACORN artifact suppression type 3. These spectra are close to the quality that would be measured on the ground.

19. Select **Save as** to save the new Atmospherically Corrected Image Information.
20. Select **Save and Run** to run the correction and save the new image.

*Appendix B an example of a completed Control File Editor window used for an AVIRIS image.

Appendix

Appendix A

Available Puerto Rico AVIRIS Scenes:

South Coast 1: f040819101p00r06
South Coast 2: f040819t01p00r09
Vieques 1 : f0408 19t01p00r07
Vieques 2: f040819t0 lp00r08
Mayaguez 1 : f0408 I 9t0 1p00r04
Mayaguez 2 : f0408 I 9t0 I p00r05
Mayaguez 3 : f0408 1 910 lp00rl 0
North Coast: f0408 19t01p00r1

	South Coast 1	**South Coast 2**	**Vieques 1**	**Vieques 2**
Year	2004	2004	2004	2004
Date	Aug 19	Aug 19	Aug 19	Aug 19
GMT	13:36:45.487	14:18:38.864	13:54:33.719	14:4:1.523
AST	9:36:45.487	10:18:39.864	9:54:33.719	10:4:1.523
Sens.Alt. (km)	20130	20094	20307	20063
Sens. Hd. (d)	86.917	267.968		256.159
Subsurf. (deg)	26.310	21.252		
Samples	677	677	677	677
Lines	10024	8403	2537	2082
Geo-Samples	1099	1098	709	705
Geo-Lines	9305	9169	2300	2263
Center Lat.	17:56:52 N	17:56:58 N	18:6:1 N	18:9:17 N
Center Long.	66:32:19 W	66:30:15 W	65:26:4 W	65:25:29 W

Notes: Atlantic Standard Time (Puerto Rico) : UTC/GMT - 4 hours

	Mayaguez 1	**Mayaguez 2**	**Mayaguez 1**	**North Coast**
Year	2004	2004	2004	2004
Date	Aug 19	Aug 19	Aug 19	Aug 19
GMT	13:12:46.838	13:22:32.040	14:32:52.362	14:48:43.814
AST	9:12:46.838	9:22:32.040	10:32:52.362	10:48:43.814
Sens.Alt. (km)	20165	20162	20106	20202
Sens. Hd. (d)	82.958	267.226	7.397	92.261
Samples	677	677	677	677
Lines	2838	2439	4212	11128
Geo-Samples	926	905	870	1137
Geo-Lines	2688	2668	4224	10345
Center Lat.	18:14:25 N	18:11:15 N	18:12:11 N	18:28:34 N
Center Long.	67:13:20 W	67:10:35 W	67:13:9 W	66:24:59 W

Appendix B:

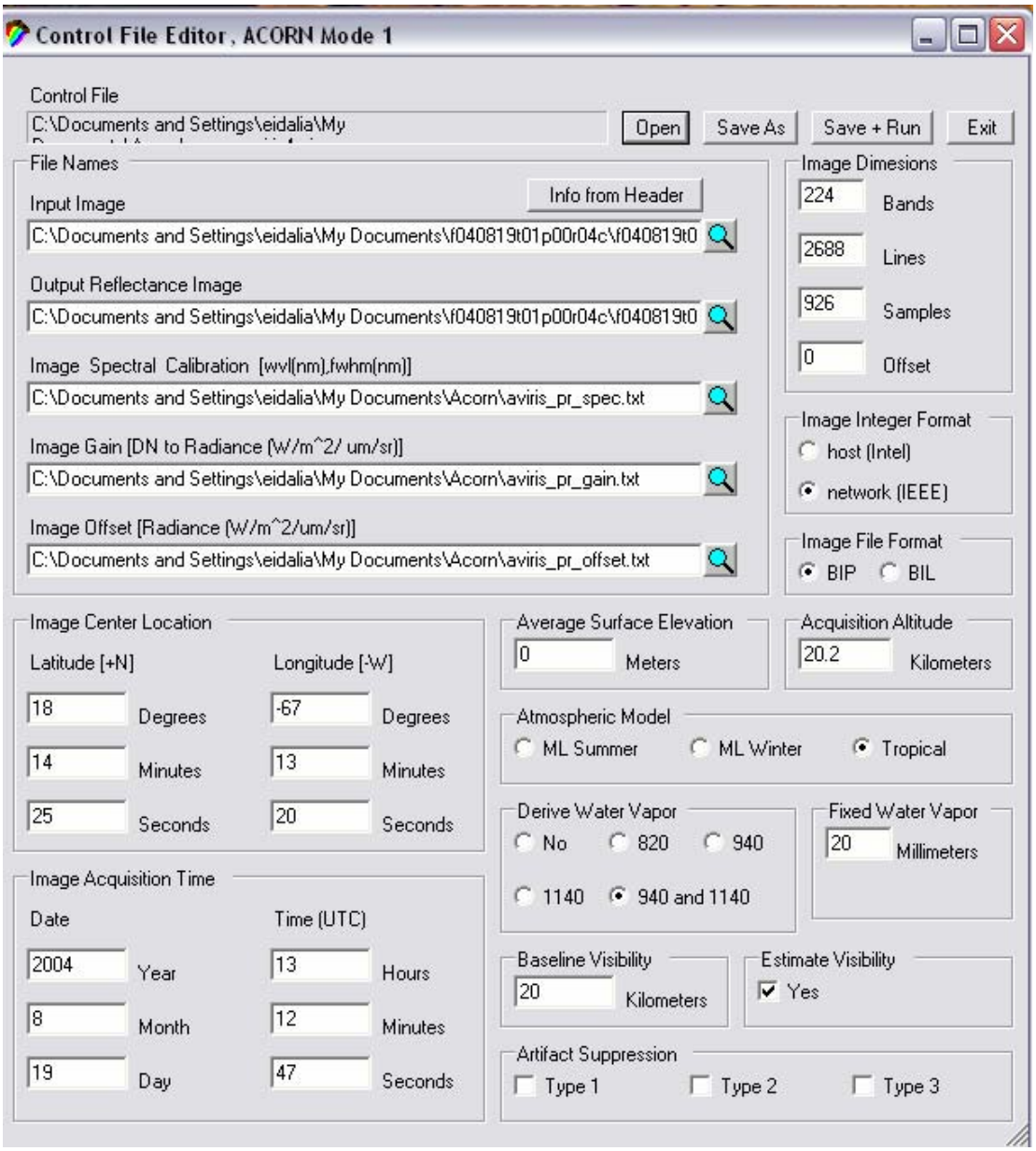
Control File Editor, ACORN Mode 1
Control File
C:\Documents and Settings\eidalia\My
Open
Save As
Save + Run
Exit
File Names
Input Image
Info from Header
C:\Documents and Settings\eidalia\My Documents\f040819t01p00r04c\f040819t0
Output Reflectance Image
C:\Documents and Settings\eidalia\My Documents\f040819t01p00r04c\f040819t0
Image Spectral Calibration [wvl(nm),fwhm(nm)]
C:\Documents and Settings\eidalia\My Documents\Acorn\aviris_pr_spec.txt
Image Gain [DN to Radiance (W/m^2/ um/sr)]
C:\Documents and Settings\eidalia\My Documents\Acorn\aviris_pr_gain.txt
Image Offset [Radiance (W/m^2/um/sr)]
C:\Documents and Settings\eidalia\My Documents\Acorn\aviris_pr_offset.txt
Image Dimesions
224 Bands
2688 Lines
926 Samples
0 Offset
Image Integer Format
host (Intel)
network (IEEE)
Image File Format
BIP
BIL
Image Center Location
Latitude [+N]
Longitude [-W]
18 Degrees
14 Minutes
25 Seconds
-67 Degrees
13 Minutes
20 Seconds
Average Surface Elevation
0 Meters
Acquisition Altitude
20.2 Kilometers
Atmospheric Model
ML Summer
ML Winter
Tropical
Image Acquisition Time
Date
Time (UTC)
2004 Year
8 Month
19 Day
13 Hours
12 Minutes
47 Seconds
Derive Water Vapor
No
820
940
1140
940 and 1140
Fixed Water Vapor
20 Millimeters
Baseline Visibility
20 Kilometers
Estimate Visibility
Yes
Artifact Suppression
Type 1
Type 2
Type 3